DOI: 10.1002/adfm.200600491

Conductive Mesocellular Silica–Carbon Nanocomposite Foams for Immobilization, Direct Electrochemistry, and Biosensing of Proteins**

By *Shuo Wu*, *Huangxian Ju*,* and *Ying Liu*

A mesocellular silica–carbon nanocomposite foam (MSCF) is designed for the immobilization and biosensing of proteins. The as-prepared MSCF has a highly ordered mesostructure, good biocompatibility, favorable conductivity and hydrophilicity, large surface area, and a narrow pore-size distribution, as verified by transmission electron microscopy (TEM), IR spectroscopy, electrochemical impedance spectroscopy (EIS), nitrogen adsorption–desorption isotherms, pore size distribution plots, and water contact angle measurements. Using glucose oxidase (GOD) as a model, the MSCF is tested for immobilization of redox proteins and the design of electrochemical biosensors. GOD molecules immobilized in the mesopores of the MSCF show direct electrochemistry with a fast electron transfer rate ($14.0 \pm 1.7\ s^{-1}$) and good electrochemical performance. Based on a decrease of the electrocatalytic response of the reduced form of GOD to dissolved oxygen, the proposed biosensor exhibits a linear response to glucose concentrations ranging from 50 μM to 5.0 mM with a detection limit of 34 μM at an applied potential of –0.4 V. The biosensor shows good stability and selectivity and is able to exclude interference from ascorbic acid (AA) and uric acid (UA) species that always coexist with glucose in real samples. The nanocomposite foam provides a good matrix for protein immobilization and biosensor preparation.

1. Introduction

Over the last two decades considerable attention has been paid to the development of new biocompatible materials with good conductivity,[1,2] suitable hydrophilicity,[1] high porosity,[3] and large surface area[4] for protein immobilization. The electrochemical biosensing applications of such materials have been explored due to the inherent advantages of electrochemical methods, such as low cost, portability, high sensitivity, and good selectivity.[5] Inorganic materials are attractive for protein immobilization due to their chemical and thermal stability, good mechanical strength, biocompatibility, and their potential for improving the stability of the enzymes and/or proteins under extreme conditions.[6,7] Ordered mesoporous materials are a typical example of inorganic materials that have been used for this purpose. These materials have high surface areas, large pore volumes, and narrow pore size distributions. Up till now, several different kinds of mesoporous molecular sieves composed of silicates,[8,9] metal oxides,[10] and carbon[11–13] have been used for protein immobilization; these materials generally exhibit excellent performance. The chemical composition, surface characteristics,[9,14] morphology,[15] as well as the mesopore distribution,[16] can be designed to improve the biocompatibility and hydrophilicity of the materials for the immobilization of different proteins. Among these mesoporous materials, mesoporous silicates are the most extensively used biocompatible materials in the area of electrochemical biosensing. Many heme proteins such as hemoglobin, myoglobin, horseradish peroxide, and cytochrome c show direct electron transfer in a series of mesoporous silica materials.[3,4,17]

Mesoporous carbon is another important versatile material due to its low cost and conductive properties. In recent years, many researchers have tried to immobilize proteins in ordered mesoporous carbon materials.[11–13,18] However, very few reports have focused on the electrochemical biosensing applications of these materials due to their limited pore diameters of less than 5 nm and their high hydrophobicity.[12,19] The hydrophobicity makes it difficult for analytes[1] in aqueous solution to approach the active enzyme sites on the electrode surface. In this work, we have designed a new mesoporous silica–carbon nanocomposite foam (MSCF) by combining the advantages of mesoporous carbon with the good biocompatibility and hydrophilicity of silica materials.

Porous silica–carbon nanocomposites have been developed as solar energy absorbers by two general strategies which lead to different carbon cluster sizes. Silica is used as a transparent binder and carbon nanoparticles are employed as the light-ab-

[*] Prof. H. X. Ju, Dr. S. Wu, Y. Liu
Key Laboratory of Analytical Chemistry for Life Science
Ministry of Education of China
School of Chemistry and Chemical Engineering
Nanjing University
Nanjing 210093 (P.R. China)
E-mail: hxju@nju.edu.cn

[**] We gratefully acknowledge the National Science Funds for Distinguished Young Scholars (20 325 518) and Creative Research Groups (20 521 503), the Key Program (20 535 010) from the National Natural Science Foundation of China, and the Creative Program for Postgraduates in Jiangsu Universities for financial support of this research. Supporting Information is available online from Wiley InterScience or from the author.

sorbing components in these materials.[20] The hybrid material, prepared using a porous silica template and a carbon precursor that is transformed into elemental carbon by a carbonization reaction, is composed of 4 nm worm-like pores interconnected by even smaller bottleneck channels. The small bottleneck channels limit the entrance of most redox proteins into the mesopores for biosensing applications. A mesocellular carbon–aluminosilicate hybrid material has also been synthesized as an intermediate product during the preparation of mesocellular carbon.[21] However, the large amount of alumina present in the nanocomposites is disadvantageous for the immobilization of proteins due to the adsorption of water in the vacancies and pore surfaces of alumina.[4] Moreover, it is difficult to preserve the bioactivity of the immobilized proteins due to the strong acidic sites introduced by alumina,[21] which can result in the unfolding of the secondary structure of the proteins due to strong electrostatic interactions.[22] Here, the MSCF is prepared by impregnating furfuryl alcohol as a carbon source into a mesocellular silica foam (MSF) template, followed by polymerization of the carbon source with the aid of a small amount of organic acid and carbonization under an inert environment. This process is performed with simple immersion instead of heating under a static vacuum environment and excludes water adsorption in the mesopores. The catalytic acidic sites of the loaded organic acid used for the polymerization of the carbon source can be easily removed during carbonization, and thus does not affect the biocompatibility of the MSCF.

The as-prepared MSCF is characterized by an ordered mesostructure, a large surface area, and an ordered mesopore size distribution. For practical purposes, the mesopore size can be controlled by changing the pore size of the MSF template.[23] Furthermore, the hydrophilicity and conductivity of the material can be changed by adjusting the relative amounts of carbon and silica, thereby enabling the immobilization and biosensing of different proteins. Using glucose oxidase (GOD) as a model, the MSCF has been used for the immobilization of proteins in the mesostructured cells by physical adsorption. The MSCF provides a desirable microenvironment where the bioactivity of GOD is retained. The immobilized GOD shows fast direct electrochemistry corresponding to its FAD/$FADH_2$ (FAD: flavin adenine dinucleotide) redox couple; we have utilized this behavior to construct a new glucose biosensor. The proposed biosensor shows a wide linear response and good stability and selectivity. Thus the MSCF nanocomposites provide an efficient strategy and a novel promising platform for the further study of direct electron transfer in proteins with implications for the development of biosensors.

2. Results and Discussion

2.1. Characteristics of the MSCF Nanocomposite

Transmission electron microscopy (TEM) images of the MSCF show uniformly distributed mesostructured cells with a diameter of 20 nm (Fig. 1a), indicating the formation of an or-

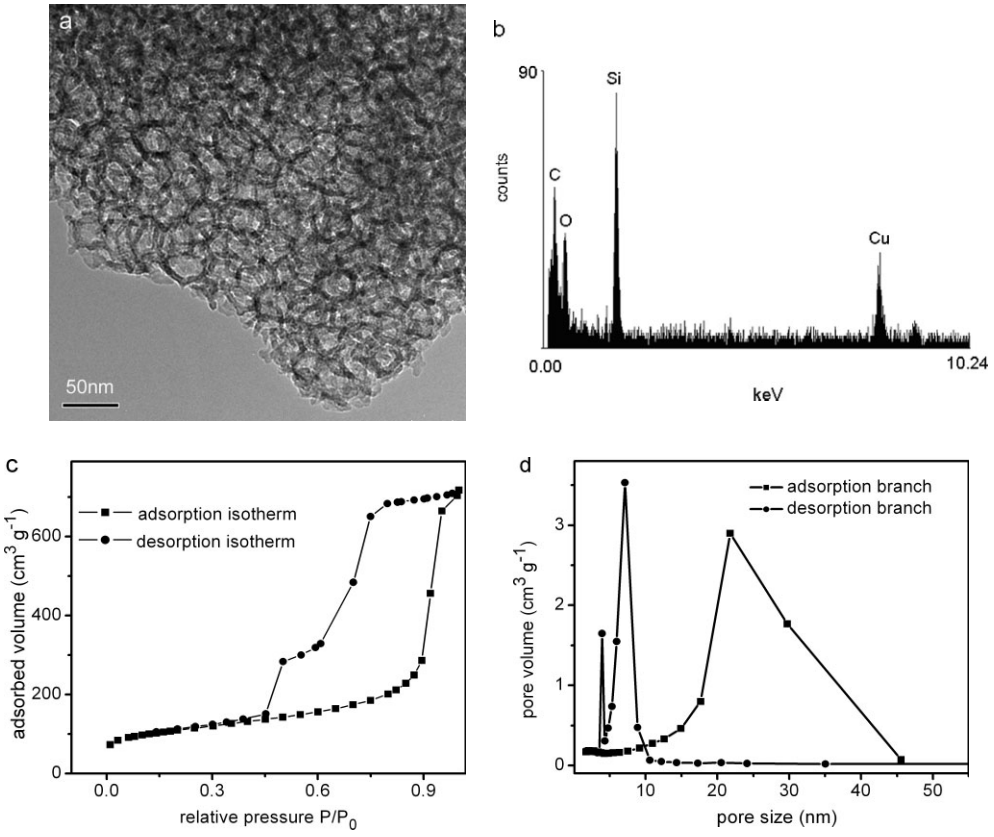

Figure 1. a) TEM image, b) EDX spectrum, c) nitrogen adsorption–desorption isotherms, and d) pore size distributions of the MSCF.

ADVANCED FUNCTIONAL MATERIALS

dered mesocellular structure. The corresponding energy-dispersive X-ray (EDX) spectrum suggests that the MSCF is only composed of biocompatible C and SiO_2 (Fig. 1b). The Cu observed in the EDX spectrum arises from the Cu grid on which the sample is placed. The N_2 adsorption–desorption isotherms of the material exhibit large hysteresis with sharp adsorption and desorption branches at high relative pressures (Fig. 1c), indicating the narrow pore size distribution of the large mesopores. The desorption branch also shows some hysteresis at relatively low pressures, indicating the presence of small mesopores. The pore size distribution can be calculated from the adsorption and desorption branches of the isotherms using the Barrett–Joyner–Halenda method, as shown in Figure 1d. Clearly, the MSCF displays two kinds of mesopores; the pore size distribution plots are centered at 7 and 20 nm, indicating that these structures possess ink-bottle-like pores.[21] Thus the MSCF is composed of main cells with a diameter of 20 nm interconnected by 7 nm windows. The window diameter of 7 nm is a good match for the dimensions of GOD molecules (7.0 nm × 5.5 nm × 8.0 nm).[7] Once the GOD molecules enter the main cells through the interconnected pores, desorption from the main cells is expected to be difficult due to the relatively large dimensions of these molecules. The MSCF also possesses small mesopores centered at around 3.7 nm arising from the replication of the MSF template;[23] these pores have not been fully occupied by the carbon source.

The Brunauer–Emmett–Teller (BET) surface area of the MSCF has been calculated to be 386 $m^2 g^{-1}$, which is less than that of conventional mesoporous materials[4,21,23] due to the filling of the complementary pores by carbon. However, these complementary pores are micropores, and thus the filling of these pores does not influence the loading of protein molecules in the mesoporous cells.[11]

Figure 2 shows the electrochemical impedance spectroscopy (EIS) data for 10 mM $Fe(CN)_6^{3-/4-}$ in 1.0 M KCl for bare-, mesocellular-carbon-foam (MCF)-, single-walled carbon nanotube (SWNT)-, multiwalled carbon nanotube (MWNT)-, MSF-, and MSCF-modified glassy carbon electrodes (GCE). The electron-transfer resistances at these modified electrodes range from 20–30 Ω, except for the MSF-modified GCE. The resistance values are lower than that of the bare GCE, indicating that the MSCF possesses good conductivity similar to MCF, SWCNTs, and MWCNTs, which is a direct result of the impregnation of conductive carbon into the complementary pores.

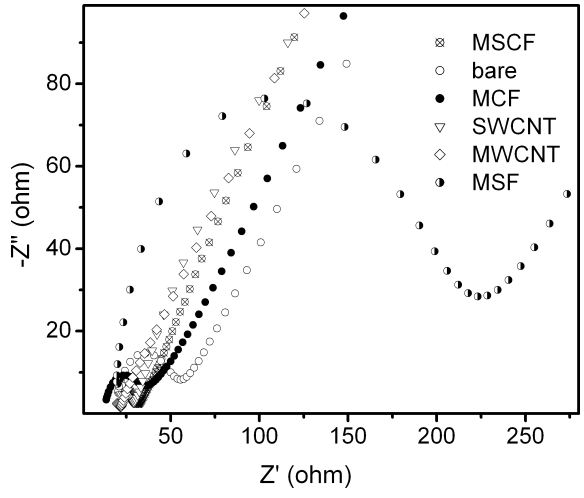

Figure 2. Electrochemical impedance spectroscopy measurements of 10 mM $Fe(CN)_6^{3-/2-}$ in 1.0 M KCl using bare, MCF-, SWNT-, MWNT-, MSCF-, and MSF-modified glassy carbon electrodes.

The water contact angle of the MSCF is 32.6°, which is similar to the 30.3° value observed for mesoporous silicates (SBA-15), and much less than the 79.1° value observed for pure carbon mesoporous materials.[19] Thus the presence of silicates greatly improves the hydrophilicity of the nanocomposite, which enables the analytes to approach the active enzyme sites.[1] Furthermore, the improvement in hydrophilicity enhances the biocompatibility of the nanocomposites for the immobilization of proteins, thereby preserving their natural structure and bioactivity.

2.2. Impregnation of GOD into the MSCF Nanocomposite

Figure 3a shows the nitrogen adsorption–desorption isotherms of the MSCF before and after impregnation of GOD with different initial concentrations. The amount of nitrogen adsorbed decreases after the immobilization of GOD. With increasing initial concentration of GOD, both the BET surface area and the pore volume decrease, as shown in Table 1. These decreases indicate that GOD molecules have entered the mesopores of the MSCF.

Table 1. Textural properties of MSCFs with different GOD loadings.

Initial GOD concentration [mg mL^{-1}]	GOD loading [wt % MSCF]	BET surface area [$m^2 g^{-1}$]	Total pore volume [$cm^3 g^{-1}$]
0	0	386	1.11
2	18.3	159	0.646
4	31.7	145	0.536
7	45.3	121	0.487

The adsorption isotherm of GOD in the MSCF is shown in Figure 3b. With increasing GOD concentration the amount of loaded GOD increases, reaching a maximum value at a GOD concentration of 5 mg mL^{-1}. Notably, the GOD adsorption isotherm is not of the Langmuir type, suggesting that the GOD immobilization mechanism is based on the entrapment of enzymes in the mesopores of the MSCFs, rather than on the adsorption of enzymes on the external surface.[18] Interestingly, the average maximum GOD adsorption amount of 44.8 ± 1.2 % (in terms of wt % of the MSCF, $n = 4$, where n = times of detection) is slightly higher than the 39.1 ± 0.7 % value observed for mesocellular carbon foams (MSU-F-C),[18] even though the BET surface area of the MSCF is less than that of MSU-F-C due to a lower abundance of micropores, which contribute little to GOD loading.

The interaction between the MSCF and GOD molecules can be studied by comparing the IR spectra of the MSCF, pure

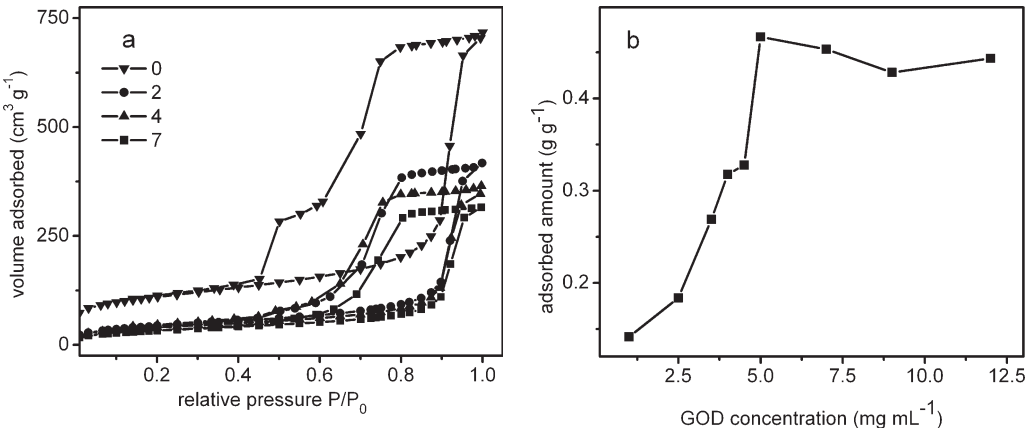

Figure 3. a) Nitrogen adsorption–desorption isotherms of MSCF samples before and after impregnation with different initial concentrations of GOD, and b) GOD adsorption isotherm obtained by incubating 10 mg of the MSCF with a GOD solution under stirring at room temperature for 48 h.

GOD, and GOD-immobilized MSCF (Fig. 4). The spectra for pure GOD molecules is characterized by two IR absorption bands centered at 1648 and 1544 cm^{-1}, which are the typical amide I and amide II absorption bands of protein molecules, respectively.[11] After loading on the MSCF, the two absorption

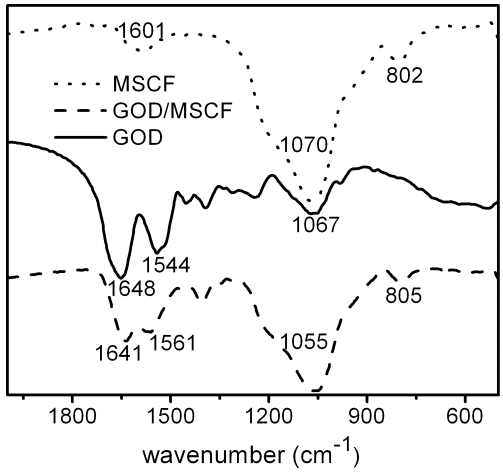

Figure 4. IR spectra of the MSCF, pure GOD, and GOD-loaded MSCF.

peaks shift to 1641 and 1561 cm^{-1}, which may be due to the strong electrostatic interactions between the charged amino acid residues on the surfaces of the protein molecules and the silanol groups on the mesoporous structure; these shifts may also arise from hydrophobic interactions between protein molecules and carbon. In general, the disappearance of the amide II absorption band is used to follow the unfolding and denaturation of the immobilized protein. The retention of this absorption band indicates that the interactions between the MSCF and GOD molecules do not change the structure of the protein. The IR spectrum of the MSCF shows absorption bands centered at 1601, 1070, and 805 cm^{-1}. The peak at 1601 cm^{-1} is attributed to the vibration of adsorbed water, whereas the other peaks are ascribed to the symmetric and asymmetric flexible vibrations of surface silanol groups in the mesocellular structure.[4] The observed shift of both absorption peaks of surface silanol groups further confirms the strong electrostatic interactions between these groups and the amino acid residues of the protein molecules.

2.3. Direct Electrochemistry of MSCF/GOD/Nafion-Modified Electrodes

Figure 5 shows the cyclic voltammograms of different electrodes in 0.2 M nitrogen-saturated phosphate buffered saline (PBS) solution at 100 mV s^{-1}. The MSCF/Nafion-modified electrode does not show any obvious redox peak, suggesting

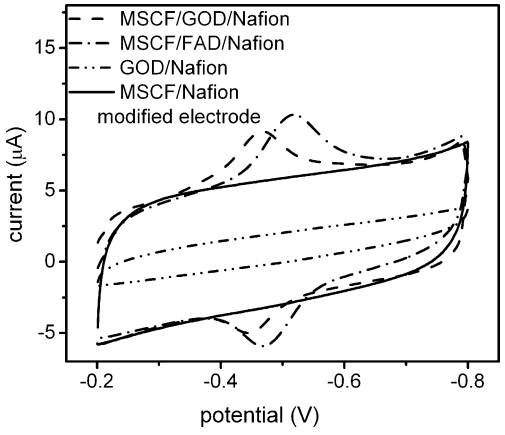

Figure 5. Cyclic voltammograms of MSCF/GOD/Nafion-, MSCF-, GOD/Nafion-, and MSCF/FAD/Nafion-modified GCEs in 0.2 M pH 7.0 PBS solutions at 100 mV s^{-1}.

that both the MSCF and the Nafion membrane are electroinactive in this potential window. After the impregnation of GOD in the MSCF, the MSCF/GOD/Nafion-modified electrode shows a pair of well-defined redox peaks at –470 and –446 mV. These peaks result from direct electron transfer at the immobilized GOD for the conversion of GOD(FAD) to

ADVANCED FUNCTIONAL MATERIALS

GOD($FADH_2$). The formal potential of GOD is –458 mV, which is very close to the standard electrode potential of –460 mV (vs. a saturated calomel electrode) for FAD/$FADH_2$ at pH 7.0 (25 °C),[24] indicating that most GOD molecules retain their native structure after impregnation in the MSCF. However, GOD/Nafion-modified electrodes do not show any peaks, which may be due to very slow electron transfer or the denaturation of GOD and ineffectiveness of Nafion in trapping GOD. Thus, the MSCF is very effective in achieving direct electron transfer at the GOD molecules. The good electrochemical response of GOD arises from two factors. One is the large space inside the mesostructured cells, which permits protein molecules to orient in conformations that are more favorable for direct electron transfer, with the active sites closer to the conducting sites. The other is the good conductivity of the MSCF matrix, which acts as an electron transfer tunnel, thereby favoring electron transfer between the protein molecules and the electrodes.

The cyclic voltammogram of the MSCF/FAD/Nafion-modified electrode shows a pair of redox peaks at –518 and –470 mV (Fig. 5), producing a formal potential of –494 mV, which is more negative than the –458 mV value observed for immobilized GOD. This difference can be rationalized by considering that the reduction of FAD groups or the oxidation of $FADH_2$ groups inside the peptides of GOD is easier or more difficult than for free FAD or $FADH_2$ because of the presence of positively charged amino acid residues of the peptides at pH 7.0.

The effect of the scan rate on the electrochemical response of impregnated GOD is shown in Figure 6a. The peak currents increase linearly with an increase of the scan rate from 100 to 300 mV s^{-1} (Fig. 6b), and the anodic and cathodic peak potentials of the impregnated GOD show shifts in positive and negative directions, respectively, indicating a surface-controlled process. From the integration of the reduction peak of the MSCF/GOD/Nafion-modified GCEs at 100 mV s^{-1}, the surface coverage of GOD is calculated to be 8.33×10^{-10} mol cm^{-2}, which is much larger than the 9.8×10^{-12} mol cm^{-2} value observed for the adsorption of GOD on gold-nanoparticle-modified carbon paste electrodes[25] and the 1.54×10^{-11} mol cm^{-2} value observed for GOD/CdS-modified electrodes.[26] The peak-to-peak separations at 200, 225, 250, 275, and 300 mV s^{-1} are 20, 23, 24, 25, and 25 mV, respectively. The small peak-to-peak separation values indicate a fast electron transfer rate. The electron transfer rate constant k_s is estimated to be 14.0 ± 1.7 s^{-1} using

$$k_s = mn\mathrm{F}v/\mathrm{R}T \quad (1)$$

when the peak-to-peak separation is less than 200 mV,[27] where m is a parameter related to the peak-to-peak separation, T is the temperature, n is the number of electrons, and v is the scan rate. This value is much larger than the corresponding values observed for GOD immobilized on MWCNT- (1.53 s^{-1}), SWCNT- (0.3 s^{-1}),[28,29] and gold-nanoparticle-modified electrodes (1.3 s^{-1}).[30] The significant increase in the electron transfer rate results from the strong interaction of GOD with the MSCF and the high conductivity of the MSCF.

The cyclic voltammograms of the MSCF/GOD/Nafion-modified electrodes show strong dependence on the pH value of the external solution (Fig. 7a). With increasing pH, the formal potential shifts negatively, exhibiting a linear relationship with a slope of 45.0 mV pH^{-1} over a pH range from 5.0 to 8.0 (Fig. 7b). This value is close to the expected value of 58 mV pH^{-1}, indicating a two-proton process coupled with a two-electron redox reaction process, which is similar to the electrode process reported previously for GOD adsorbed on colloidal gold nanoparticles (slope of 43.7 mV pH^{-1}).[25]

2.4. Biosensing Applications of the MSCF/GOD/Nafion-Modified Electrodes

Figure 8 shows the cyclic voltammograms of MSCF/GOD/Nafion-modified electrodes in nitrogen- and air-saturated 0.2 M PBS solutions with and without the addition of 1.0 mM glucose at 100 mV s^{-1}. A pair of well-resolved redox peaks can be observed in both air- and nitrogen-saturated PBS. However, the cathodic peak current is larger and the anodic peak current is lower in the air-saturated solution as compared to the corre-

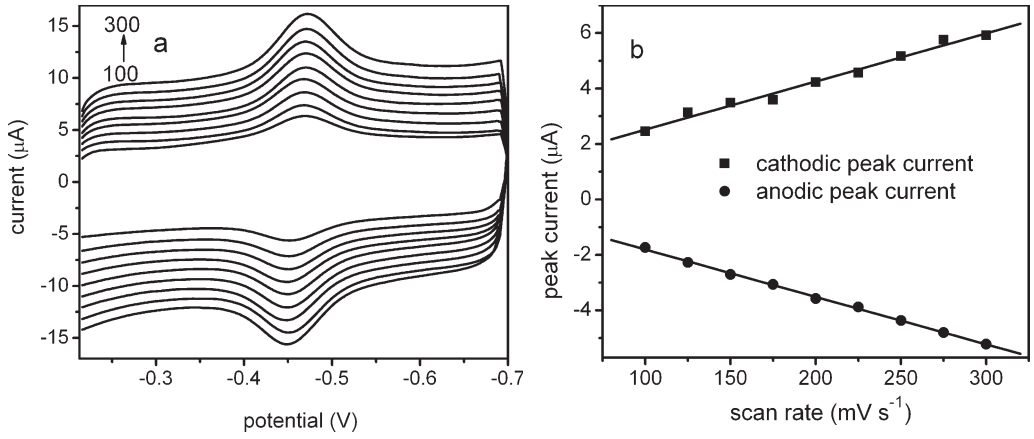

Figure 6. a) Cyclic voltammograms of a MSCF/GOD/Nafion-modified GCE in 0.2 M PBS solution at scan rates of 100, 125, 150, 175, 200, 225, 250, 275, and 300 mV s^{-1} (from bottom to top), and b) plots of the anodic and cathodic peak currents versus the scan rate.

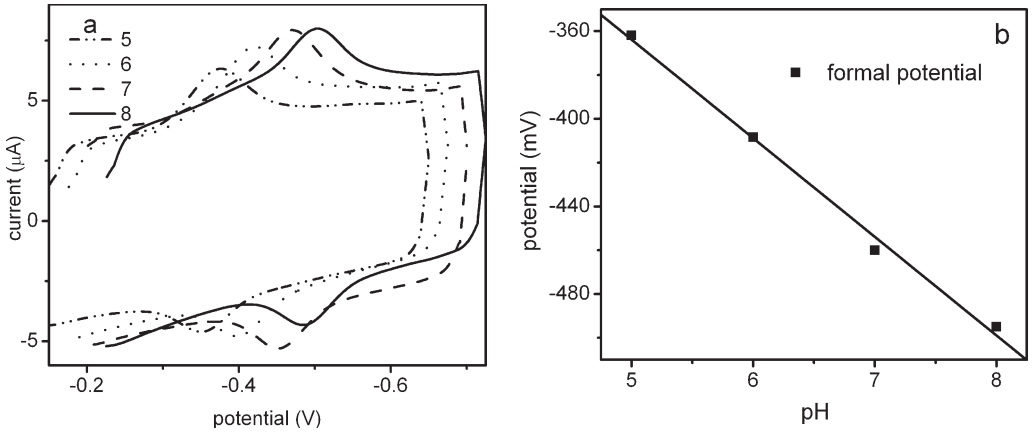

Figure 7. a) Cyclic voltammograms of MSCF/GOD/Nafion-modified GCEs in 0.2 M PBS solutions with pH values of 5.0, 6.0, 7.0, and 8.0 measured at a scanning rate of 100 mV s^{-1}, and b) plot of the formal potential versus the pH.

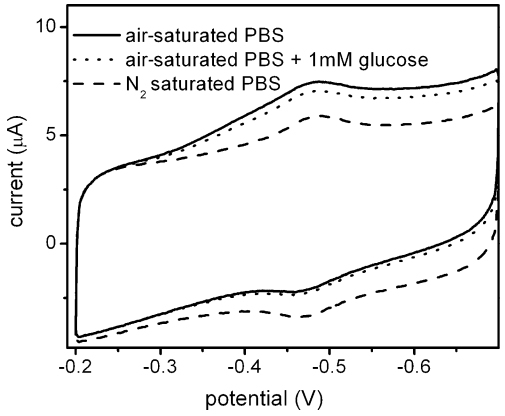

Figure 8. Cyclic voltammograms of the MSCF/GOD/Nafion-modified electrode in nitrogen- and air-saturated 0.2 M PBS solutions with and without the addition of 1.0 mM glucose. The voltammograms have been measured at a scan rate of 100 mV s^{-1}.

sponding peaks in the nitrogen-saturated solution, indicating that dissolved oxygen participates in the redox process of the immobilized GOD. In other words, the electrochemically formed GOD($FADH_2$) can electrocatalyze the reduction of dissolved oxygen.[25] Upon the addition of 1.0 mM glucose to an air-saturated 0.2 M PBS solution, the cathodic peak current decreases due to the enzymatic reaction between the oxidized form of GOD and glucose. Based on the decrease of the electrocatalytic response to dissolved oxygen, this system can be used as a glucose biosensor.

The amperometric response of the MSCF/GOD/Nafion-modified electrode to glucose starts at a potential of –0.25 V and reaches its maximum value at –0.4 V; the latter value has been used here for the amperometric detection of glucose. This applied potential appears to be more negative than those based on the consumption of dissolved oxygen,[31,32] such as carbon nanotubes immobilized on electrodes, which electrocatalytically reduce dissolved oxygen.

The influence of GOD loading on the amperometric response has been examined at –400 mV. With increasing GOD concentration used for the preparation of the modified electrode, the response increases significantly and reaches a maximum value at a GOD concentration of 4 mg mL^{-1} (Fig. S1, Supporting Information). Although maximum GOD loading is obtained at a GOD concentration of 5 mg mL^{-1}, the resulting electrode shows a lower response than that obtained at 4 mg mL^{-1}, suggesting that both the GOD amount and the remaining mesopore volume influence the response. The latter factor relates to the accessibility of the enzyme to both dissolved oxygen and glucose. At 5 mg mL^{-1} the GOD fills 56.1 % of the pore volume, whereas the corresponding value at 4 mg mL^{-1} is 51.3 %, which is low enough to allow the substrates easy access to the loaded GOD.

Figure 9a shows the amperometric response of the biosensor to successive additions of glucose for an air-saturated and stirred 0.2 M pH 7.0 PBS solution at –400 mV. Each successive addition of glucose results in a decrease in the steady-state current. The time required for reaching 95 % of the steady-state response is less than 4 s. The linear calibration range for glucose is 0.05–5.0 mM ($r = 0.999$, $n = 11$) with a detection limit of 35 μM. The linear range of up to 5.0 mM is comparable to that observed for the electrocatalytic reduction of dissolved oxygen by MWCNTs,[31] is larger than the 2 mM limit for oxygen-sensitive glucose biosensors,[32,33] and is indeed much larger than the 0.28 mM value based on the same mechanism for gold-nanoparticle-modified electrodes.[25] Such an extended linear range arises from the increased oxygen content around the immobilized GOD due to the large surface area and mesoporous volume of the MSCF.

To assess the stability of the immobilized enzyme, the MSCF/GOD/Nafion-modified electrodes have been scanned continuously in a 0.2 M pH 7.0 PBS solution. Upon continuous sweeping the voltammetric response decreases very slowly (Fig. S2, Supporting Information). After scanning for 80 cycles the decrease in the peak current is less than 8 %, indicating good stability. When ten MSCF/GOD/Nafion-modified elec-

ADVANCED FUNCTIONAL MATERIALS

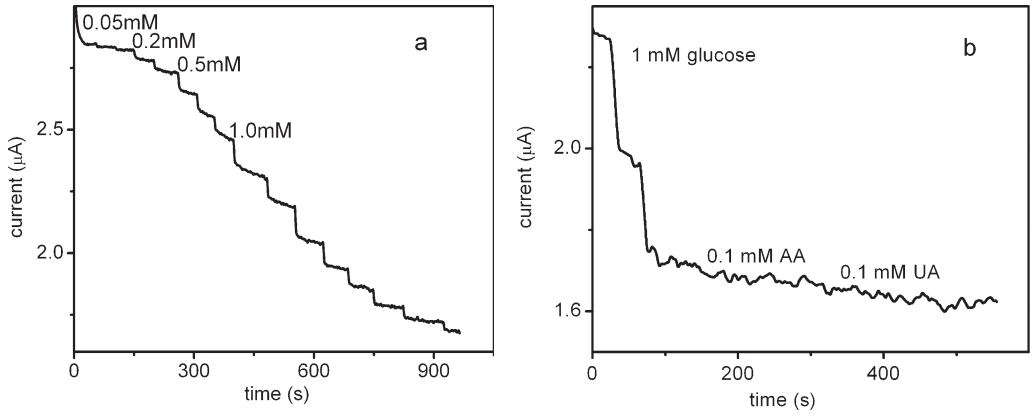

Figure 9. a) Current–time curve of the MSCF/GOD/Nafion-modified electrode for successive additions of specific concentrations of glucose to air-saturated and stirred 0.2 M pH 7.0 PBS solutions at –400 mV, and b) effect of interfering species on the biosensor response.

trodes are sequentially stirred in 2 mL water for 30 min, no GOD is detectable in the resulting solution by UV-vis spectrometry, suggesting that the leaching of GOD is negligible. The good retention of the GOD is due to the bottleneck-like structure of the MSCF[18] and the strong interaction between GOD molecules and the MSCF.

The biosensor also shows good selectivity for glucose. In an air-saturated and stirred 0.2 M pH 7.0 PBS solution containing 1.0 mM glucose, the response arising from 0.1 mM uric acid (UA) and ascorbic acid (AA) is negligible (Fig. 9b). When the biosensor is stored at 4 °C in 0.2 M PBS, it retains 94 % of its initial current response towards glucose after intermittent use over a 2 week period, further corroborating that the biosensor is stable and that the MSCF is efficient at retaining the activity of the enzyme. The intra-assay coefficient of variation for six repeated determinations of 1.0 mM glucose is 3.1 %, indicating acceptable precision (Fig. S3, Supporting Information). The inter-assay coefficient of variation for five measurements of 1.0 mM glucose using five independently prepared electrodes is 5.1 %, indicating good fabrication reproducibility.

3. Conclusions

In this work, we demonstrate a MSCF for protein immobilization and biosensing applications. The MSCF exhibits favorable conductivity for electron transfer, good and tunable hydrophilicity, and biocompatibility for protein immobilization. The natural structure and bioactivity of the protein is preserved in the MSCF. Moreover, the MSCF is characterized by a large surface area for loading the protein and a uniform pore size distribution that is appropriate for the size of the protein. The as-prepared MSCF shows an ink-bottle-like mesostructure with 20 nm main cells interconnected by 7 nm pores. The IR spectra of GOD molecules impregnated in the MSCF provide evidence for the preservation of the protein structure and the strong electrostatic interactions between silanol groups in the foams and the charged amino acid residues on the protein surfaces. The impregnated GOD molecules show fast direct electrochemistry, confirming the role of carbon in improving the conductivity of the composites. A glucose sensor has been developed based on the decrease of the electrocatalytic response of the reduced form of GOD to dissolved oxygen. The biosensor displays excellent analytical performance over a wide linear range along with good stability and selectivity. Interference from AA and UA that usually coexist with glucose in real samples has been found to be negligible. All these characteristics suggest that MSCF nanocomposites are good biocompatible materials, and are suitable for protein impregnation and the preparation of third-generation biosensors.

4. Experimental

Materials: GOD (Type α-S, from Aspergillus niger, 39.8 U mg^{-1}), FAD, β-D(+)-glucose, Nafion, and trimethylbenzene were purchased from Sigma-Aldrich (USA). Furfuryl alcohol was purchased from Fluka (Germany). SWCNTs and MWCNTs were purchased from Shenzhen Nanotech Port. Poly(ethylene oxide)-*block*-poly(propylene oxide)-*block*-poly(ethylene oxide) ($EO_{20}PO_{70}EO_{20}$, Pluronic P123) was purchased from BASF (Germany). All other reagents were of analytical grade and used without further purification. A 0.2 M PBS solution was prepared by mixing stock solutions of NaH_2PO_4 and Na_2HPO_4. Doubly distilled water was used in all the experiments.

Preparation of the MSCF and SBA-15: MSF was synthesized as reported previously in the literature [23], and was used as a template. The MSCF was prepared as follows: 1 g of the MSF was immersed in a 2 mL acetone solution containing 0.02 g paratoluenesulfonic acid (PTS) with stirring for 2 h, followed by evaporation of the acetone to obtain the PTS-loaded template (PTS–MSF). Furfuryl alcohol was then impregnated into the PTS–MSF template by an immersion step. After filtration, furfuryl-alcohol-impregnated PTS–MCF was polymerized at 373 K for 2 h. The unpolymerized furfuryl alcohol was then extracted at 523 K under vacuum. The obtained composite was further heated at 1173 K under flowing nitrogen for 5 h in order to carbonize the carbon source. The resulting product was the MSCF. As a control, SBA-15 was synthesized according to a method previously reported in the literature [34]. MCF was prepared by etching the obtained MSCF with HF to remove the MSF template.

GOD Adsorption: A series of GOD solutions were prepared by dissolving different amounts of GOD in 0.2 mM pH 7.0 PBS solutions. The GOD concentrations were determined by UV absorption at 280 nm to range from 1 to 12 mg mL^{-1}. UV-vis spectra were collected on a Shimadzu UV-3600 UV-vis spectrophotometer (Japan). In each adsorption

experiment, 10 mg of the MSCF was suspended in 2.7 mL of the appropriate GOD solution. The resulting mixture was continuously shaken in a shaking bath at room temperature for 48 h. The GOD loading was calculated by subtracting the amount remaining in the supernatant liquid after adsorption from the initial amount of GOD.

Preparation of MSCF/GOD/Nafion- and MSCF/FAD/Nafion-Modified Electrodes: GCEs (3 mm in diameter, CH Instruments, USA) were first polished to a mirror finish using 0.3 and 0.05 μm alumina slurries (Beuhler), followed by thorough rinsing with deionized water. After sonicating successively in a 1:1 (v/v) nitric acid/water solution, acetone, and deionized water, the electrodes were dried at room temperature. 10 mg of the MSCF was added into 5 mL water and stirred for 2 h to obtain the MSCF suspension. 3 μL of the 2 mg mL^{-1} MSCF suspension, 4 mg mL^{-1} GOD (in 0.2 M pH 7.0 PBS solution), and 0.5 % Nafion were subsequently placed on the pretreated GCE surface and allowed to dry under ambient conditions for 2 h after each drop-casting step. The formed Nafion membrane was used to fix the GOD-impregnated MSCF nanoparticles on the electrode surface. In the case of FAD as a control, 3 μL 5 μg mL^{-1} FAD was used in place of the GOD solution to prepare the MSCF/FAD/Nafion-modified electrode.

Apparatus: TEM observations were conducted on a JEOL JEM-2010 (Japan) electron microscope at an accelerating voltage of 200 kV. The microscope was equipped with EDX spectroscopy capabilities (Vantage DS, USA) for analyzing the various components of the MSCF. Nitrogen adsorption–desorption isotherms and pore size distributions (calculated by the Barrett–Joyner–Halenda method) were measured at 77 K using a Micrometeritics ASAP 2020 system. The GOD-impregnated MSCF for nitrogen adsorption–desorption analysis was prepared by dispersing 0.12 g of the MSCF in 60 mL GOD solutions with different initial concentrations for 4 h, followed by centrifugation to remove the unadsorbed protein. The samples were outgassed for 10 h at 200 °C before the measurements. The static water contact angle was measured at 25 °C using drops of deionized water on the surfaces of the samples. The IR spectra were obtained using a Vector 22 spectrometer. All electrochemical measurements were performed on a CHI 660B electrochemical workstation (CH Instruments, USA) with a conventional three-electrode system comprising a platinum wire as an auxiliary, a saturated calomel electrode as the reference, and modified GCEs as the working electrodes. The amperometric detection of glucose and the electrocatalytic measurements were carried out in air-saturated solutions. Other electrochemical experiments were performed in solutions deoxygenated by bubbling highly pure nitrogen for 15 min. These solutions were maintained under a nitrogen atmosphere during measurements.

Received: June 6, 2006
Revised: August 11, 2006
Published online: January 24, 2007

[1] S. Sampath, O. Lev, *Anal. Chem.* **1996**, *68*, 2015.
[2] V. B. Kandimalla, V. S. Tripathi, H. X. Ju, *Biomaterials* **2006**, *27*, 1167.
[3] Z. H. Dai, X. X. Xu, H. X. Ju, *Anal. Biochem.* **2004**, *332*, 23.
[4] Z. H. Dai, S. Q. Liu, H. X. Ju, H. Y. Chen, *Biosens. Bioelectron.* **2004**, *19*, 861.
[5] P. C. Pandey, S. Upadhyay, I. Tiwari, S. Sharma, *Electroanalysis* **2001**, *13*, 1519.
[6] A. M. Klibanov, *Science* **1983**, *219*, 722.
[7] M. Hartmann, *Chem. Mater.* **2005**, *17*, 4577.
[8] J. F. Díaz, K. J. Balkus Jr., *J. Mol. Catal. B: Enzymatic* **1996**, *2*, 115.
[9] Y. Han, S. Lee, J. Ying, *Chem. Mater.* **2006**, *18*, 643.
[10] X. Xu, Z. B. Tian, J. L. Kong, S. Zhang, B. H. Liu, D. Y. Zhao, *Adv. Mater.* **2003**, *15*, 1932.
[11] A. Vinu, M. Miyahara, K. Ariga, *J. Phys. Chem. B* **2005**, *109*, 6436.
[12] A. Vinu, C. Streb, V. Murugesan, M. Hartmann, *J. Phys. Chem. B* **2003**, *107*, 8297.
[13] M. Hartmann, A. Vinu, *Chem. Mater.* **2005**, *17*, 829.
[14] H. Takahashi, B. Li, T. Sasaki, C. Miyazaki, T. Kajino, S. Inagaki, *Chem. Mater.* **2000**, *12*, 3301.
[15] J. Lei, J. Fan, C. Z. Yu, L. Y. Zhang, S. Y. Jiang, B. Tu, D. Y. Zhao, *Microporous Mesoporous Mater.* **2004**, *73*, 121.
[16] J. Deere, E. Magner, J. G. Wall, B. K. Hodnett, *Catal. Lett.* **2003**, *85*, 19.
[17] Z. H. Dai, S. Q. Liu, H. X. Ju, *Electrochim. Acta* **2004**, *49*, 2139.
[18] D. Lee, J. Lee, J. Kim, J. Kim, H. B. Na, B. Kim, C. H. Shin, J. N. Kwak, A. Dohnalkova, J. W. Grate, T. Hyeon, H. S. Kim, *Adv. Mater.* **2005**, *17*, 2828.
[19] L. F. Wang, Y. Zhao, K. F. Lin, *Carbon* **2006**, *44*, 1298.
[20] Y. Mastai, S. Polarz, M. Antonietti, *Adv. Funct. Mater.* **2002**, *12*, 197.
[21] J. Lee, K. Sohn, T. Hyeon, *J. Am. Chem. Soc.* **2001**, *123*, 5146.
[22] C. H. Lee, J. Lang, C. Y. Mou. *J. Phys. Chem. B* **2005**, *109*, 12 277.
[23] P. Schmidt-Winkel, W. W. Lukens, P. D. Yang, D. I. Margolese, J. S. Lettow, J. Y. Ying, G. D. Stucky, *Chem. Mater.* **2000**, *12*, 686.
[24] I. Tinoco, K. Kauer, J. C. Wang, *Physical Chemistry—Principles and Applications in Biological Sciences*, Prentice-Hall, Englewood Cliffs, NJ **1978**, p. 606.
[25] S. Q. Liu, H. X. Ju, *Biosens. Bioelectron.* **2003**, *19*, 177.
[26] Y. X. Huang, W. J. Zhang, H. Xiao, G. X. Li, *Biosens. Bioelectron.* **2005**, *21*, 817.
[27] E. Laviron, *J. Electroanal. Chem.* **1979**, *101*, 19.
[28] C. X. Cai, J. Chen, *Anal. Biochem.* **2004**, *332*, 75.
[29] J. Q. Liu, A. Chou, W. Rahmat, *Electroanalysis* **2005**, *17*, 38.
[30] S. Zhao, K. Zhang, Y. Bai, W. W. Yang, C. Q. Sun, *Bioelectrochemistry* **2006**, *69*, 158.
[31] H. T. Zhao, H. X. Ju, *Anal. Biochem.* **2006**, *350*, 138.
[32] Y. Q. Dai, K. K. Shiu, *Electroanalysis* **2004**, *16*, 1697.
[33] T. Rinken, T. Tenno, *Biosens. Bioelectron.* **2001**, *16*, 53.
[34] D. Zhao, J. Feng, Q. Huo, G. D. Stucky, *Science* **1998**, *279*, 548.